Testing the capability of ORCHIDEE land surface model to simulate Arctic ecosystems: Sensitivity analysis and site-level model calibration

Sarah Dantec-Nédélec, Catherine Ottle, Wang Tao, F. Guglielmo, Fabienne Maignan, Nicolas Delbart, V. Valdayskikh, T. Radchenko, O. Nekrasova, Jean Jouzel

AGU PUBLICATIONS

Journal of Advances in Modeling Earth Systems

RESEARCH ARTICLE

10.1002/2016MS000860

Key Points:
- The ORCHIDEE land surface model is calibrated and evaluated at local scale for two sites typical of Arctic environments (forest and shrub-tundra)
- A global sensitivity analysis identified the parameters having most influence on water and energy flux simulation
- Model performance and improvements provided by the vertical discretization of the soil hydrothermal properties are highlighted

Supporting Information:
- Supporting Information S1
- Figure S1
- Figure S2

Correspondence to:
C. Ottlé,
catherine.ottle@lsce.ipsl.fr

Citation:
Dantec-Nédélec, S., et al. (2017), Testing the capability of ORCHIDEE land surface model to simulate Arctic ecosystems: Sensitivity analysis and site-level model calibration, *J. Adv. Model. Earth Syst.*, *9*, 1212–1230, doi:10.1002/2016MS000860.

Received 15 NOV 2016
Accepted 28 APR 2017
Accepted article online 8 MAY 2017
Published online 18 MAY 2017

Testing the capability of ORCHIDEE land surface model to simulate Arctic ecosystems: Sensitivity analysis and site-level model calibration

S. Dantec-Nédélec[1], C. Ottlé[1], T. Wang[1], F. Guglielmo[1], F. Maignan[1], N. Delbart[2], V. Valdayskikh[3], T. Radchenko[3], O. Nekrasova[3], V. Zakharov[3], and J. Jouzel[1]

[1]LSCE-IPSL, UMR 8212, CNRS-CEA-UVSQ, Orme des Merisiers, Gif-sur-Yvette, France, [2]PRODIG, UMR 8586, Université Paris-Diderot, Paris, France, [3]Ural Federal University, Yekaterinburg, Russia

Abstract The ORCHIDEE land surface model has recently been updated to improve the representation of high-latitude environments. The model now includes improved soil thermodynamics and the representation of permafrost physical processes (soil thawing and freezing), as well as a new snow model to improve the representation of the seasonal evolution of the snow pack and the resulting insulation effects. The model was evaluated against data from the experimental sites of the WSibIso-Megagrant project (www.wsibiso.ru). ORCHIDEE was applied in stand-alone mode, on two experimental sites located in the Yamal Peninsula in the northwestern part of Siberia. These sites are representative of circumpolar-Arctic tundra environments and differ by their respective fractions of shrub/tree cover and soil type. After performing a global sensitivity analysis to identify those parameters that have most influence on the simulation of energy and water transfers, the model was calibrated at local scale and evaluated against in situ measurements (vertical profiles of soil temperature and moisture, as well as active layer thickness) acquired during summer 2012. The results show how sensitivity analysis can identify the dominant processes and thereby reduce the parameter space for the calibration process. We also discuss the model performance at simulating the soil temperature and water content (i.e., energy and water transfers in the soil-vegetation-atmosphere continuum) and the contribution of the vertical discretization of the hydrothermal properties. This work clearly shows, at least at the two sites used for validation, that the new ORCHIDEE vertical discretization can represent the water and heat transfers through complex cryogenic Arctic soils—soils which present multiple horizons sometimes with peat inclusions. The improved model allows us to prescribe the vertical heterogeneity of the soil hydrothermal properties.

1. Introduction

The Arctic is recognized as a region where present warming and the associated climatic and environmental changes are among the most pronounced [*Hinzmann et al.*, 2005]. In Siberia particularly, the recorded temperature changes are the largest within the Northern Hemisphere, with average winter temperatures increasing by more than 2°C and summer temperatures by 1.35°C since 1881, as reported by [*Groisman and Soja*, 2009]. This large sensitivity to global warming is explained by the specific features of the Siberian climate that is strongly affected by its proximity to the Arctic Ocean, by the sea ice changes and by the related feedbacks. Indeed, north of the Eurasian coast, sea ice thickness has noticeably reduced [*Frolov et al.*, 2009] and the Arctic Ocean is rapidly moving toward ice-free conditions each summer [*Koenigk et al.*, 2013]. The end-of-summer ice extent has reduced by half since the late 1970s [*Serreze et al.*, 2007]. These changes dramatically affect the surface albedo, the heat fluxes to the atmosphere and, thus, the regional atmospheric circulation and the advection of warmer air masses over northern Eurasia; changes which also explain the high variability of Siberian climate [*Groisman et al.*, 1994]. These positive feedbacks, added to the continental ones linked to snow, permafrost, soil moisture, albedo, and species competition [*Chapin et al.*, 2005; *Lorantу and Goetz*, 2012], may further exacerbate the situation and lead to amplification of the greenhouse warming [*Koven et al.*, 2011]. These effects have been predicted by the general circulation models (GCM) or Earth system models (ESM) involved in the Coupled Model Intercomparison Project CMIP5 [*Koenigk et al.*, 2013; *Dufresne et al.*, 2013; *Koven et al.*, 2013]. These models simulate the air temperature over Siberia

increasing by up to 6°C for the higher greenhouse gases emission scenarios (RCP8.5) [*Koenigk et al*., 2013]. However, large differences were observed among the models due to their different levels of complexity; the number of processes and feedbacks represented; and their ability to represent permafrost processes [*Dankers et al*., 2011; *Koven et al*., 2013; *Slater and Lawrence*, 2013; *Paquin and Sushama*, 2015]. The impact of climate forcing on the predictions of soil warming rate and permafrost degradation was also highlighted by *Peng et al*. [2016], who used nine process-based ecosystem models forced by different observation-based climates during the period 1960–2000. Their results allowed them to show that the climate forcing uncertainties contribute to a larger spread of soil temperature warming trends than the uncertainty of model structures. Given such features, it is clearly necessary to reduce the spread of the future projections by further developing the ESMs to include better representation of the biogeophysical processes and their interactions, and to evaluate them at various scales using less uncertain meteorological forcing data [*Chadburn et al*., 2015].

Much work has been dedicated in the past to the understanding and representation of the continental feedback processes in the ORCHIDEE (Organizing Carbon and Hydrology In Dynamic Ecosystems) land surface model used in the ESM developed at the "Institute Pierre Simon Laplace (IPSL)" [*Hourdin et al*., 2006]. Recent developments have improved the representation of snow processes with a new discretization of the snowpack into three layers [*Wang et al*., 2013] replacing the single-layer model used previously. Previous work has demonstrated that this three-layer representation gives a better simulation of the energy transfers in the snowpack and of the insulation effects through a more accurate representation of the snow thermal conductivity. Snowmelt and sublimation processes have also clearly been improved, since the multilayer snow module can simulate refreeze-thaw events in the snowpack, water transfer between snow layers and has a realistic parameterization of the aerodynamic roughness of snow surfaces. Freeze-thaw processes have also been the subject of recent developments with the inclusion of a new soil freezing scheme designed to represent the latent heat exchanges induced by soil water phase change [*Gouttevin et al*., 2012]. The soil freezing scheme introduced into ORCHIDEE considerably improves the representation of run-off and river discharge in regions underlain by permafrost or subject to seasonal freezing. More recently, *Wang et al*. [2016] implemented new soil thermodynamics with a common vertical discretization for soil moisture and thermodynamics, allowing us to prescribe varying hydrothermal soil properties with depth. Peat layers for example, with high soil water holding and heat capacities, but low heat conductivity, could be mimicked, even if the current parametrization of mineral soils only accounts for quartz, water, and other mineral materials.

The new discretization scheme, which is common to both soil moisture and temperature, also models the heat transfers linked to water diffusion. These capabilities should allow it to better represent the complexity of cryoturbated soils which present multiple horizons with different soil properties resulting from the repeated freeze/thaw cycles.

This paper discusses the capability of this new version of the ORCHIDEE land surface model to represent the water and heat transfers in Arctic environments, after evaluation against data from two instrumented sites located in a continuous permafrost area, especially instrumented for the WSibIso-Megagrant project (www.wsibiso.ru). The specific objectives of our study were first to identify the dominant physical processes and the corresponding model parameters at play in cold conditions through a global sensitivity analysis, and second to evaluate the model including the cryosphere processes against in situ measurements of soil humidity, soil temperature and active layer thickness (ALT, i.e., the top soil layer which freezes/thaws seasonally). In the following, the study area and the model and data used are first presented (sections 2 and 3). The model sensitivity analysis presented in section 4 then allows us to perform a model calibration and evaluation using data from two experimental sites (section 5). The results are discussed in section 6.

2. Study Area and Observations

The study area is part of the Labytnangi Ecological Research Station (66°39′N, 66°24′E), which is situated in the Tyumen region of Russia (Yamalo-Nenets Autonomous District) on the left/west bank of the Ob River, the westernmost of the three great Siberian rivers that flow into the Arctic Ocean (Figure 1). The station is located 18 km from Salekhard, the closest town to the polar circle, situated on the opposite side of the Ob River. The region is situated in the continuous permafrost area with a subarctic climate. The average annual

Figure 1. Study area location (the town of Labytnangi in Yamal Peninsula is indicated by a red star). The political map of Russia was obtained from http://vidiani.com (© 2011 Vidiani.com, political map of Russia).

temperature and precipitation are −7°C and 400 mm, respectively. The maximum annual snow depth rarely exceeds 1 m, with a snow season duration of approximately 220 days beginning mid-October and ending around mid-May. The landscape is flat and the soils are formed on layered sediments of the Quaternary period [*Valdayskikh et al*., 2013]. The experimental area is located in the forest-tundra area of the Yamal Peninsula, a transitional zone between the tundra zone further north and the warmer forest (taiga) zone to the south (see Figure 2, provided by the ESA-CCI Land cover project) [*Bontemps et al*., 2013]. The forested areas are mainly composed of needleleaf deciduous trees with lower fractions of needleleaf evergreen and broadleaf deciduous species. The shrubby tundra zone begins 10 km to the north of the site, with the vegetation becoming more sparse with increasing latitude.

The Labytnangi research station belongs to the INTERACT network (International Network for terrestrial Research and monitoring in the Arctic) and was established in 1954, driven by two main aims: (i) to conduct ecological investigations on a year-round basis and (ii) to create a logistics base for the core activities of the Institute of Plant and Animal Ecology.

This region was chosen to monitor vegetation dynamics and understand the impacts of climate change on boreal ecosystems. For that purpose, six key sites have been identified for vegetation mapping, each site is characteristic of a typical vegetation ecosystem encountered in the Arctic, i.e., tundra (herbaceous and shrubs), wetlands, and forests [*Valdayskikh et al*., 2013]. The main data collected comprise vegetation species, abundance, community structure, phenology and productivity, soil pedology properties, and permafrost ALT. A meteorological station was installed in July 2012 and four out of the six sites were equipped with soil temperature and soil moisture sensors. In addition, for all sites except for the forest site, soil samples as well as soil moisture and swamp water were analyzed for water isotopes. Such data can be used to constrain the representation of surface processes in land surface models [*Guglielmo et al*., 2015]. In this study, we worked only on the two sites presenting continuous data sets of both soil temperature and moisture during summer 2012, the two other sites equipped were unfortunately, strongly affected by instrument issues leading to important gaps in the data acquisition record. The first site, referred to hereafter as "Forest," is situated on a stratified sandy loamy soil characterized by high thermal conductivity and high hydraulic diffusivity. The vegetation is composed of larch and birch trees, with shrubs, and lichens in the first 2 cm of soil. The second site, called "Tundra," is characterized by a silt loamy soil covered by dwarf shrubs (mostly needleleaf summergreen), mosses and lichens. The soil

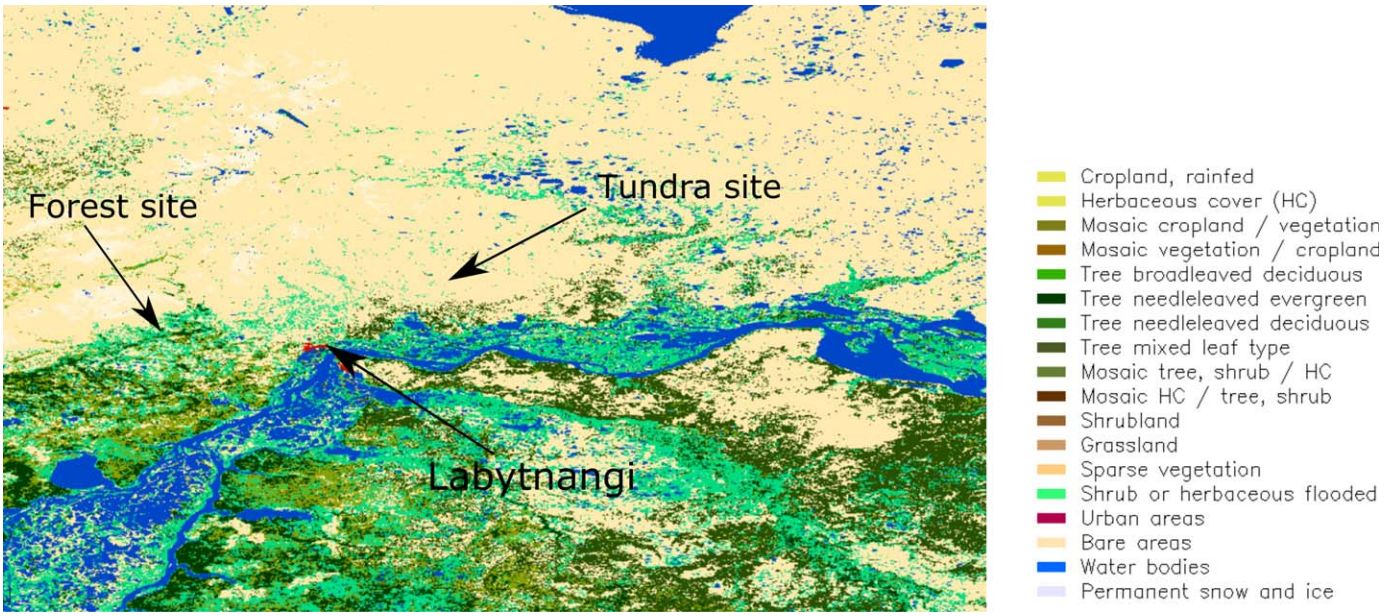

Figure 2. Land-cover map (ESA CCI product) [*Bontemps et al*., 2013] around Labytnangi and locations of the two experimental sites (Tundra and Forest).

presents a complex structure, characterized by low values of the thermal conductivity and low values of hydraulic diffusivity. The first 10 cm of soil are rich in organic matter with a deep layer of mosses with sphagnum on top. These two sites were equipped with automatic sensors (Decagon Devices, Pullman, WA) for monitoring soil temperature and moisture; these sensors were installed at the end of July 2012 at fixed depths of 2, 10, 20, and 50 cm, data were collected with a sampling frequency of 10 min. In the forest site, a supplementary sensor was installed at a depth of 100 cm, whereas for the tundra site, the deepest sensor was located at the top of the permafrost (70 cm). Data precision has been estimated from the analysis of the standard deviation of the high frequency measurements. It shows that the uncertainty on soil temperature measurements is about ± 0.1 K. For soil moisture, the precision is equal to ± 0.01 m^3 m^{-3} but decreases to ± 0.08 m^3 m^{-3} when the temperature is around the freezing point.

The ALT was assessed in the two studied sites by measuring thaw depths using small-diameter metal 3 m length rods inserted to reach the bottom of the active layer. One hundred samples were acquired at random positions in the tundra and slightly more (121 samples) in the forest site. In the tundra, the top of the permafrost was found at a depth of 60–75 cm; whereas in the forest, it could not be assessed with the 3 m probes; this could indicate that our site is located on a talik.

3. ORCHIDEE Model

The ORCHIDEE land surface model is a mechanistic dynamic global vegetation model [*Krinner et al*., 2005] that is part of the "Institut Pierre Simon Laplace (IPSL)" Earth System Model (ESM) [*Dufresne et al*., 2013]. It is composed of three main modules: SECHIBA [*Ducoudré et al*., 1993], which calculates energy, momentum and hydrological exchanges between soil, vegetation and atmosphere as well as photosynthesis, at a half-hourly time step; STOMATE which simulates carbon processes such as litter decomposition, carbon allocation and phenology, at daily time step; and LPJ [*Sitch et al*., 2003] which represents the vegetation dynamics at annual time step. ORCHIDEE is built on the concept of PFTs (Plant Functional Types) to describe vegetation distribution. Species with similar characteristics are grouped together and the model distinguishes 12 PFTs (tropical evergreen and deciduous forests, temperate broadleaf evergreen and deciduous forests, temperate needleleaf forest, boreal needleleaf evergreen and deciduous forests, boreal broadleaf deciduous forest, natural C3 and C4 grasslands, and C3 and C4 crops) plus bare soil. In the ORCHIDEE standard version, the PFTs are distributed according to two databases, the AVHRR IGBP 1 km global land-cover map [*Belward et al*., 1999] and the *Olson et al*. [1983] biome classification,

which comprises 96 land types. The PFT map prescribes the fraction of each PFT at a spatial resolution of 5 km [*Vérant et al*., 2004]. Thus, different PFTs can coexist in every grid element, and their fraction can vary if the dynamic vegetation submodule LPJ [*Sitch et al*., 2003] is activated. Recently, this PFT classification has been revised by *Ottlé et al*. [2013] to improve the mapping of boreal ecosystems, based on higher resolution satellite land-cover mapping such as the European Space Agency (ESA) GLOBCOVER 2005 [*Bicheron et al*., 2006]. This new product was used here to prescribe PFT fractions for both studied sites. The hydrological and thermal physical processes in the standard version of the model include the new soil freezing/thawing module [*Gouttevin et al*., 2012] based on an 18-layer discretization reaching 90 m for the thermal processes and an 11-layer discretization of the 2 m soil hydrology [*de Rosnay et al*., 2002]. The new snow model of intermediate complexity [*Wang et al*., 2013], based on a vertical discretization of three layers, is also included. Evaluation against local and large scale (satellite) estimates of surface temperature, ALT, freezing/thawing indices, soil moisture, snow water equivalent, albedo, to name but a few, allows to demonstrate the merits of these developments [*Gouttevin et al*., 2012; *Wang et al*., 2013]. In this work, we have also tested an improved soil thermodynamics scheme implemented by *Wang et al*. [2016] to represent various soil horizons. A new vertical discretization common to both soil moisture and soil temperature calculation was defined: see *Wang et al*. [2016, Figure 2]. This submodel is based on a multilayer scheme with a geometric progression of the internode distance from the first node at a depth of 5×10^{-4} m to the last one at depth 65.5 m (when 18 layers are prescribed, their respective depths (in meter) are the following: 0.0005, 0.002, 0.006, 0.014, 0.03, 0.06, 0.12, 0.25, 0.5, 1, 1.75, 2.5, 3.5, 5.5, 9.5, 17.5, 33.5, and 65.5). In this study, since the objectives are focused on water and thermal processes at short time scales, we run the SECHIBA module with prescribed vegetation conditions derived from in situ measurements.

3.1. Model Parameters

The ORCHIDEE standard version includes a large number of parameters whose values must be prescribed before running the model. In SECHIBA, we identified 48 parameters controlling soil hydrology and thermal processes as well as snowpack evolution. Among them, 6 parameters are related to soil albedo, 19 to snow mechanical and thermal properties, 11 to soil hydrological transfers, 5 to soil thermal processes, and 7 to vegetation properties determining energy and evapotranspiration processes (see Table 1 for a complete description of the parameters).

3.2. Model Input Data and Experimental Setup

The atmospheric input data required to run ORCHIDEE consist of continuous (6-hourly) time series of surface air temperature and humidity, pressure, wind speed, precipitation, and shortwave and longwave downward radiation. All these variables are recorded at the WMO-standard meteorological station of Salekhard (see section 2) except precipitation and radiation. For these missing data, ERA-INTERIM reanalysis data were downloaded and merged to complete the data set [*Guglielmo et al*., 2015]. Soil type and PFT fractions are also required for stand-alone simulations. These parameters were defined for the two studied sites according to in situ measurements [*Valdayskikh et al*., 2013], the PFT fractions were derived following the combination rules proposed by *Ottlé et al*. [2013]. These fractions are listed in Table 2. The seasonal variations of the LAI (Leaf Area Index) of the vegetation, required for computing the water and energy fluxes (including photosynthesis processes), are estimated daily according to the subsoil temperature as proposed by *Dickinson et al*. [1993]. This parametrization led to maximum values of LAI of 2 for the tundra and 3 for the forest site with a start of season occurring at the end of May. Finally, initial conditions of the state variables need to be assigned to run ORCHIDEE. For that purpose, and in order to reach equilibrium, the model is run on a spin-up period of a few years (e.g., 10 years if only water and energy budgets and not soil carbon are considered). In permafrost areas, since the thermal processes are calculated on a deeper soil than normal to capture the multidecadal temperature variability shown by *Nicolsky et al*. [2007], the spin-up has to be extended in time and generally 100 years are required to reach equilibrium. In our case, since we were looking only at surface processes and because only 1 year of local meteorological data was available, we decided to use the ERA-INTERIM reanalysis (already used to gap-fill the local meteorological data set) to generate our initial conditions. For that purpose, the 10 last years (2002–2011) were chosen, and the initial states were obtained after running the model iteratively ten times over this 10 year period. The surface temperature profile was initialized with a deep temperature (90 m), set to 272 K, according to the mean air temperature provided by the ERA data set over

Table 1. ORCHIDEE Parameters Used in the Sensitivity Analysis (the Morris Method), the Definition, Reference Value, and Range of Variation Are Listed for the Two Studied Sites

Parameter	Definition	Reference	Range of Variation	
		Tundra	Forest	
Soil Albedo Values to Soil Color Classification				
α_{VD}	Dry bare soil albedo values in visible range	0.18	0.18	20%
α_{ND}	Dry bare soil albedo values in near-infrared range	0.36	0.36	20%
α_{VW}	Wet bare soil albedo values in visible range	0.0	0.09	20%
α_{NW}	Wet bare soil albedo values in near-infrared range	0.18	0.18	20%
α_{LV}	Leaf albedo of vegetation type, visible albedo	0.1	0.78	20%
α_{LN}	Leaf albedo of vegetation type, near-infrared albedo	0.29	0.26	20%
Snow Albedo				
α_{snow_max}	Maximum snow albedo	0.85	0.7–1.0	
α_{snow_min}	Minimum snow albedo	0.50	0.3–0.6	
τ_a	Albedo decay rate for dry snow	0.008	20%	
τ_f	Albedo decay rate for wet snow	0.24	20%	
z_{0n}	Snow roughness length (m)	0.001	0.0001–0.01	
rw_{min}	Snow holding capacity 1	0.03	20%	
rw_{max}	Snow holding capacity 2	0.10	20%	
ρ_{snow}	Snow density (kg m^{-3})	200	20%	
Snow Thermal Properties				
a_λ	Snow thermal conductivity parameter (W m^{-2} K^{-1})	0.02	20%	
b_λ	Snow thermal conductivity parameter (W m^5 K^{-1} kg^{-2})	2.5×10^{-6}	20%	
$a_{\lambda v}$	Snow thermal conductivity (vapor) parameter (W m^{-1} K^{-1})	−0.06023	20%	
$b_{\lambda v}$	Snow thermal conductivity (vapor) parameter (W m^{-1})	−2.5425	20%	
$c_{\lambda v}$	Snow thermal conductivity (vapor) parameter (K)	−289.99	20%	
a_{sc}	Snow settling parameter (s^{-1})	2.8×10^{-6}	20%	
b_{sc}	Snow settling parameter (K^{-1})	0.04	20%	
c_{sc}	Snow settling parameter (m^3 kg^{-1})	460.0	20%	
η	Snow Newtonian viscosity parameter (Pa s^{-1})	3.7×10^7	20%	
a_η	Snow Newtonian viscosity parameter (K^{-1})	0.081	20%	
b_η	Snow Newtonian viscosity parameter (m^3 kg^{-1})	0.018	20%	
Soil Hydrological Parameters				
		Tundra	Forest	
n	Van Genuchten water retention curve coeff. n	1.56	1.89	10%
A	Van Genuchten water retention curve coeff. a (mm^{-1})	0.0036	0.0075	50%
θ_r	Residual soil water content (m^3 m^{-3})	0.078	0.065	20%
θ_s	Saturated soil water content (m^3 m^{-3})	0.46	0.44	20%
K_s	Hydraulic conductivity saturation (mm d^{-1})	249.6	1060.8	50–3000
P_{CENT}	Soil moisture above which transpiration is max	0.5	0.5	20%
θ_f	Volumetric water content field capacity (m^3 m^{-3})	0.29	0.29	20%
θ_w	Volumetric water content wilting point (m^3 m^{-3})	0.15	0.15	20%
MC_{AWET}	Volumetric water content above which albedo is constant	0.25	0.25	20%
MC_{ADRY}	Volumetric water content below which albedo is constant	0.1	0.1	20%
ψ_s	Matrix potential at saturation (mm)	−300	−300	20%
Vegetation Parameters				
$C_{ROOT\ s}$	Root profile coefficient/PFT	0, 0.8, 0.8, 1, 0.8, 0.8, 1, 1, 0.8, 4, 4, 4, 4	20%	
$V_{w\ min}$	Minimum wind speed (m s^{-1})	0.1	20%	
Z_{0s}	Bare soil roughness length (m)	0.01	20%	
LAI	Leaf Area Index	0, 8, 8, 4, 4.5, 4.5, 4, 4.5, 4, 2, 2, 2, 2	20%	
LAI_{min}	Minimum Leaf Area Index	0, 8, 0, 4, 4.5, 0, 4, 0, 0, 0, 0, 0, 0	20%	
H_v	Height of vegetation (m)	0, 50, 50, 30, 30, 30, 20, 20, 20, 0.2, 0.2, 0.4, 0.4	20%	
Rk_v	Structural resistance (s m^{-1})	0.0, 25.0, 25.0, 25.0, 25.0, 25.0, 25.0, 25.0, 25.0, 2.5, 2.0, 2.0, 2.0	20%	
Soil Thermal Parameters				
C_D	Dry soil heat capacity of soils (J m^{-3} K^{-1})	1.80×10^6	20%	
λ_D	Dry soil heat conductivity of soils (W m^{-2} K^{-1})	0.40	20%	
C_W	Wet soil heat capacity of soils (J m^{-3} K^{-1})	3.03×10^6	20%	
λ_W	Wet soil heat conductivity of soils (W m^{-2} K^{-1})	1.89	20%	
FR_{DT}	Freezing window (K)	2	1–3	

the period (1960–1990). We have checked, that even if the deep soil temperatures are warmly biased by a few Kelvin (between 2 and 3 K for our two sites) compared with a spin-up generated on a longer run of meteorological data, as long as only water and energy transfers are concerned, there is no impact on the soil temperatures and processes in the first meter of soil.

Table 2. Soil Type and PFT Fractions Prescribed for the Forest and Tundra Sites

Soil and Vegetation Parameters	Forest	Tundra
PFT TYPE (Fractions)		
PFT 1 (bare soil)	0.006	0
PFT 8 (broadleaf summergreen)	0.014	0.036
PFT 9 (needleleaf summergreen)	0.522	0.084
PFT 10 (C3 grass)	0.458	0.88
Texture (Fractions)	Sandy Loam	Silty Loam
Sand	0.65	0.2
Silt	0.3	0.65
Clay	0.05	0.15

4. Sensitivity Analysis

Among all the ORCHIDEE parameters, some are physically based and their values are derived from observations (ground based or satellite), others are conceptual and have been calibrated globally to correctly reproduce water and energy fluxes to the atmosphere. When the model is run at local scale or when new output variables are evaluated, these parameters require local calibration. Model calibration is a difficult task and can be achieved by various optimization approaches designed to minimize the discrepancies between simulated and observed variables. But the efficiency of these methods (and consequently their choice) depends greatly on the number of parameters involved. If too many parameters are searched, the optimization process may be underdetermined. Therefore, it is essential, prior to the calibration step, to identify those parameters that have most influence on the output variables constrained by the available observations. This problem may be solved by applying sensitivity analysis (SA) methods [*Morris*, 1991; *Sobol*, 2001; *Gubler et al*., 2013]. These methods allow us to analyze the impact of input parameters on model output variables and to assess model uncertainties. SA techniques can be divided into two categories: local or global. Local methods consist of analyzing the derivatives of the model outputs with respect to each model parameter, whereas global methods analyze the model outputs after sampling the whole parameter space. Among the methods of this latter type, we can distinguish screening methods which consist of sampling the parameter space and detecting the parameters which have no influence on the considered output variables, and importance sampling methods like variance decomposition techniques, which are more quantitative and allow ranking of the parameter sensitivities and their interactions. The second type of method is generally based on a large ensemble of simulations, which requires huge computational resources when the size of the parameter space increases. For this reason, the sensitivity analysis is often performed in two steps: in the first step the main influential parameters are selected by a screening method; in the second step their sensitivity is quantified [*Lu et al*., 2013; *Sobol*, 1990]. Therefore, we first applied a screening method [*Morris*, 1991] to qualitatively identify the parameters which are not influential on the selected output variables, thereby reducing the parameter space. In a second step, we used a variance decomposition method [*Sobol*, 2001] to quantify the model output sensitivities to the model parameters.

4.1. Parameter Sensitivity Analysis Based on the Morris Method

4.1.1. Methodology

The simplest way to perform an SA is to study the elementary effect of perturbing each parameter in a predefined range, one-factor-at-a-time (OAT) on the model output. A standard value and an uncertainty range are defined for each parameter and the variance of the model outputs is analyzed to rank the most sensitive parameters. To account for parameter interactions [*Saltelli et al*., 2008; *Campolongo et al*., 2011], the experimental plan is designed to consider all the possible parameter combinations in order to explore the entire parameter space. In the Morris method, the experimental plan OAT is repeated randomly until all parameters are perturbed within their uncertainty range. More precisely, in the case of a K-dimensional parameter space, if each model parameter $P_{i,\ (i=1,\ 2,\ 3,\ldots,\ K)}$ is sampled within an n-level discretization grid (n), the elementary effect *ee* on the output model variable *Y* due to a predefined perturbation Δ of parameter P_i can be written:

$$ee_i(Y) = \frac{Y(\ldots P_i + \Delta \ldots) - Y(\ldots P_i \ldots)}{\Delta}$$

This elementary effect is calculated for $K+1$ simulations, each corresponding to a combination of a randomly perturbed number of parameters. This plan is repeated r times with r so-called "trajectories," and these $r\times(K+1)$ model simulations allow calculation of the mean (μ) and the standard deviation (σ) of the effects obtained by perturbing each parameter. These two statistical values are then used to rank the

parameters according to their influence on the output variable, and to separate nonsensitive parameters from sensitive ones.

In our case, the Morris function was used under "R" computing environment [*Pujol et al*., 2014] with K = 48 parameters using the sampling strategy improved by *Campolongo et al*. [2007] with n = 5 levels of discretization and r = 40 trajectories. The trajectories were sampled with a revised strategy, maximizing the interdistances to optimally cover the parameter space. After computation of the elementary effects, a rescaling/normalization was performed to allow the comparison between parameters.

4.1.2. Application and Results of the Morris Analysis

The SA experiments were performed for the two sites with three model output variables: the top (0–15 cm) soil temperature and soil moisture, and ALT which was calculated as the maximum depth of the thawed layer during our simulation period. These variables were chosen because they were measured on-site. The prescribed parameter ranges (Table 1) were set for most parameters to 20% of the reference value following previous SA studies [*Wang et al*., 2013; *Kuppel et al*., 2013; *Benavidès Pinjosovsky et al*., 2017], except for the physical parameters like the ones related to the hydrological pedotransfer, for which the ranges were defined according to literature analysis [*Carsel and Parrish*, 1988].

The SA was performed on simulations over the year 2012 with the surface conditions, i.e., the soil and vegetation (PFT) fractions, defined in Table 2. The analysis was done seasonally because we expected the parameter ranking to vary from one season to the other, according to the time-varying dominant biophysical processes. Indeed, we expected snow parameters to be more influential in winter and spring, and soil hydrological ones to impact primarily summer water transfers. The four seasons studied were defined as follows: spring (April–June), summer (July–September), fall (October–December), and winter (January–March). Because similar results were obtained for both sites, we present here only those obtained on the Tundra site.

Figure 3 presents the results obtained for the Tundra site, for the four seasons and the three output variables selected. The horizontal bars represent the normalized elementary effects (in percentages) calculated for the 48 model parameters. They were obtained by averaging the absolute values of the elementary effects calculated for the whole experimental plan OAT.

It can be seen that the sensitivities vary greatly among the parameters and in time. The intercomparison allows us to differentiate three cases: the parameters which are not sensitive whatever the season (for example, the soil field capacity θ_f that appears nonsensitive probably because of the low fractions of vegetation cover prescribed), those which are sensitive to at least one variable (like the snow roughness length Z_{0n}, that affects mostly the ALT) or one season (an example is the Van Genuchten *n* retention curve coefficient), and those which are sensitive to all the output variables or during the whole year (like the soil thermal conductivity and heat capacity). Since our final goal is a model calibration on summer soil moisture and soil temperature observations, we decided to keep only the parameters that are especially sensitive in summer on the three output variables. A threshold of 35% for the normalized elementary effects was empirically defined to select the most influential parameters which were kept for the second step of the SA, that in which we analyze more quantitatively the parameters' influence and interactions with a larger number of simulations and a variance-based analysis. This threshold allows us to reject 38 parameters and to keep the 10 most sensitive ones that are listed in Table 3. We can see that the parameters kept are related to soil heat conduction, soil evaporation, water diffusion, and soil freezing. Only 2 snow parameters (snow albedo and thermal conductivity) among the 19 ones appear still sensitive in summer, this is because of the delay effects of snow insulation and snowmelt on soil temperature and moisture.

4.2. Parameter Sensitivity Analysis Based on the Sobol' Indices

4.2.1. Methodology

As already noted, the Morris method allows us to determine which input parameters exert the most influence on the model output variables, and which parameters can be discarded in a calibration process. The method provides a global parameter sensitivity ranking but does not allow us to discern whether the variance of the effects of a parameter is due to model nonlinearities or to parameter interactions [*Lu et al*., 2013]. That information would be helpful for defining a calibration strategy and can be assessed by decomposing the variance, through ANOVA (Analysis of Variance). This approach consists of decomposing the

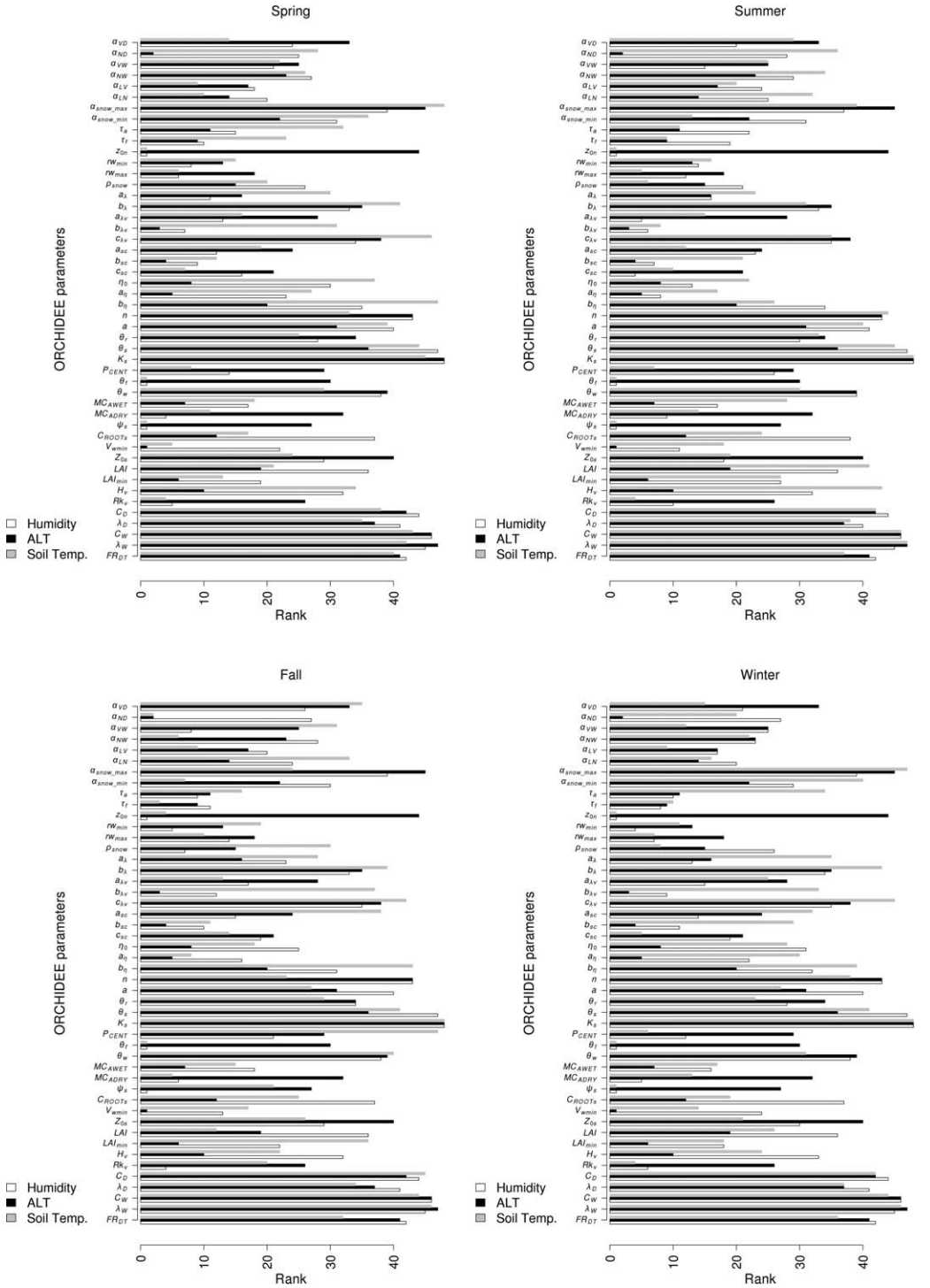

Figure 3. ORCHIDEE parameter ranking based on the Morris method applied to soil moisture, soil temperature, and active layer thickness (ALT) for the four seasons (spring, summer, fall, and winter) and for the Tundra site.

total variance into partial variances representing the main and higher-order effects of a parameter P_i on the model output Y. Keeping the same notations introduced in section 4.1.1, the total variance of the model output Y can be written as a sum of partial variances of individual parameters and parameter interactions *Sobol'* [2001]. It can then be written:

$$V(Y)=\sum_{i=1}^{K} V_i+\sum_{i=1}^{K}\sum_{j=i+1}^{K} V_{i,j}+\sum_{i<j<l} V_{i,j,l}+\ldots+V_{i,j,l\ldots K}$$

where V_i represents the main or first-order variance contribution of the ith parameter, $V_{i,j}$, the second-order contribution of the interactions between parameters i and j when other inputs are kept constant, and $V_{1,2,\ldots,m}$ represent all the interactions higher than third order up to the K parameters.

After division of both sides of this equation by the total variance $V(Y)$, we can write a relation between partial contributions, the so-called "Sobol' sensitivity indices":

$$1=\sum_{i=1}^{K} S_i+\sum_{i=1}^{K}\sum_{j>i}^{K} S_{i,j}+\ldots+S_{i,j,l,\ldots,K}$$

In this equation, the first-order Sobol' index S_i (also called *main* effect) represents the fraction of the total model output variance explained by parameter P_i, apart from interactions with other parameters. The total-order index introduced by *Homma and Saltelli* [1996] measures the total effect of parameter P_i (i.e., sum of the main effect of parameter P_i and of all its interactions with the other model parameters). It can be shown that this total-order index can be written as a function of $V_{\sim i}$, which represents the model output variance explained by all the parameters except the one under consideration, as

$$S_{Ti}=1-\frac{V_{\sim i}}{V}$$

For nonadditive models, i.e., models with interactions between parameters, S_{Ti} is greater than S_i, and the sum of all Sobol' indices is less than 1. Therefore, the interactions between P_i and the other parameters may be assessed by analyzing the difference between S_{Ti} and S_i [*Nossent et al*., 2011].

Saltelli [2002] showed that the minimum number of simulations required to calculate robust indices is $n_d \times (K+2)$, where n_d is the number of random deviates. Here this number was set empirically to 1200 in order to carefully explore the parameter space. In our case with $K=10$ parameters, this sampling leads to 14,400 sets of parameters and simulations to perform. In the following, the calculations have been done using the methods of *Jansen* [1999] and *Saltelli et al*. [2010] to calculate the Sobol' indices, under "R" environment [*Pujol et al*., 2014].

4.2.2. Application and Results

The analysis was performed for the 10 parameters selected after the Morris step, which are listed in Table 4. First-order and total-order indices were computed; the results were analyzed by comparing the Sobol' indices seasonally, for the output variables soil moisture, temperature and ALT, as described previously.

Figures 4 and 5 present the first-order and total-order Sobol' indices calculated for the soil temperature and the soil moisture averaged over the topmost 30 cm of soil, for the four seasons, respectively. The total effect (triangles) and main effect (circles) with 95% confidence intervals (vertical lines) are plotted for each parameter. Note that sometimes the confidence interval is not visible on the plot because of its low value.

The results show that, in general, the two indices (main and total) are very close to each other for all the parameters and variables studied, which means that the parameters appear quite independent. The discrepancies are a little larger for the two hydraulic parameters, saturated soil water content Θ_s and hydraulic conductivity at saturation K_s, for which we can suspect a slight correlation. The most sensitive parameter for soil temperature is the snow thermal conductivity parameter $C_{\lambda v}$, which explains nearly 80% of the variance in fall and winter. The hydraulic parameters Θ_s and K_s are mostly sensitive in summer when the soil water transfer processes are dominant and strongly affect evapotranspiration and soil temperature. The snow albedo parameter α_{snow_max} is influential in spring because of its impact on the energy budget and snowmelt. For soil moisture, Θ_s and K_s appear to be the most sensitive parameters: Θ_s is more influential than K_s during

Table 3. ORCHIDEE Parameters Selected for the Second Step of the Sensitivity Analysis (the Sobol Method)

α_{snow_max}	Maximum snow albedo
$C_{\lambda v}$	Snow thermal conductivity (vapor) parameter (K)
n	Van Genuchten coefficient n
θ_s	Saturated soil water content ($m^3\ m^{-3}$)
K_s	Soil hydraulic conductivity at saturation (mm d^{-1})
C_D	Dry soil heat capacity (J $m^{-3}\ K^{-1}$)
λ_D	Dry soil heat conductivity (W $m^{-2}\ K^{-1}$)
C_W	Wet soil heat capacity (J $m^{-3}\ K^{-1}$)
λ_W	Wet soil heat conductivity (W $m^{-2}\ K^{-1}$)
FR_{DT}	Freezing window (K)

Table 4. ORCHIDEE Most Sensitive Parameters for the Four Seasons Studied

	Soil Moisture	Soil Temperature
Spring	θ_s, K_s	α_{snow_max}, $C_{\lambda v}$, θ_s
Summer	θ_s, K_s	θ_s, K_s
Fall	θ_s, K_s	$C_{\lambda v}$
Winter	θ_s, K_s	α_{snow_max}, $C_{\lambda v}$

summer and autumn, whereas the contrary is observed over the rest of the year. This can be explained by the seasonal variation of the partitioning between the different components of the water budget, with a larger contribution from soil evaporation during the summer and early fall snow-free period, whereas the presence of many precipitation events and the dominance of infiltration processes in winter and spring impact the runoff/drainage partitioning and explain the larger effect of K_s.

Figure 6 presents the results obtained for the third output variable under study, the ALT. As shown on the graph, most of the variance is explained by two thermal parameters, the soil thermal conductivity λ_W and heat capacity C_w for the wet soil, which take part directly in the calculation of this diagnostic variable. The snow albedo and thermal conductivity also appear sensitive but to a lesser extent, because they influence the spring soil temperatures.

In summary, the sensitivity experiments permitted us to identify the following five parameters having the most impact on ALT, soil temperature and moisture, namely: saturated soil water content Θ_s, hydraulic conductivity at saturation K_s, soil thermal conductivity λ_W, heat capacity C_w, and snow thermal conductivity

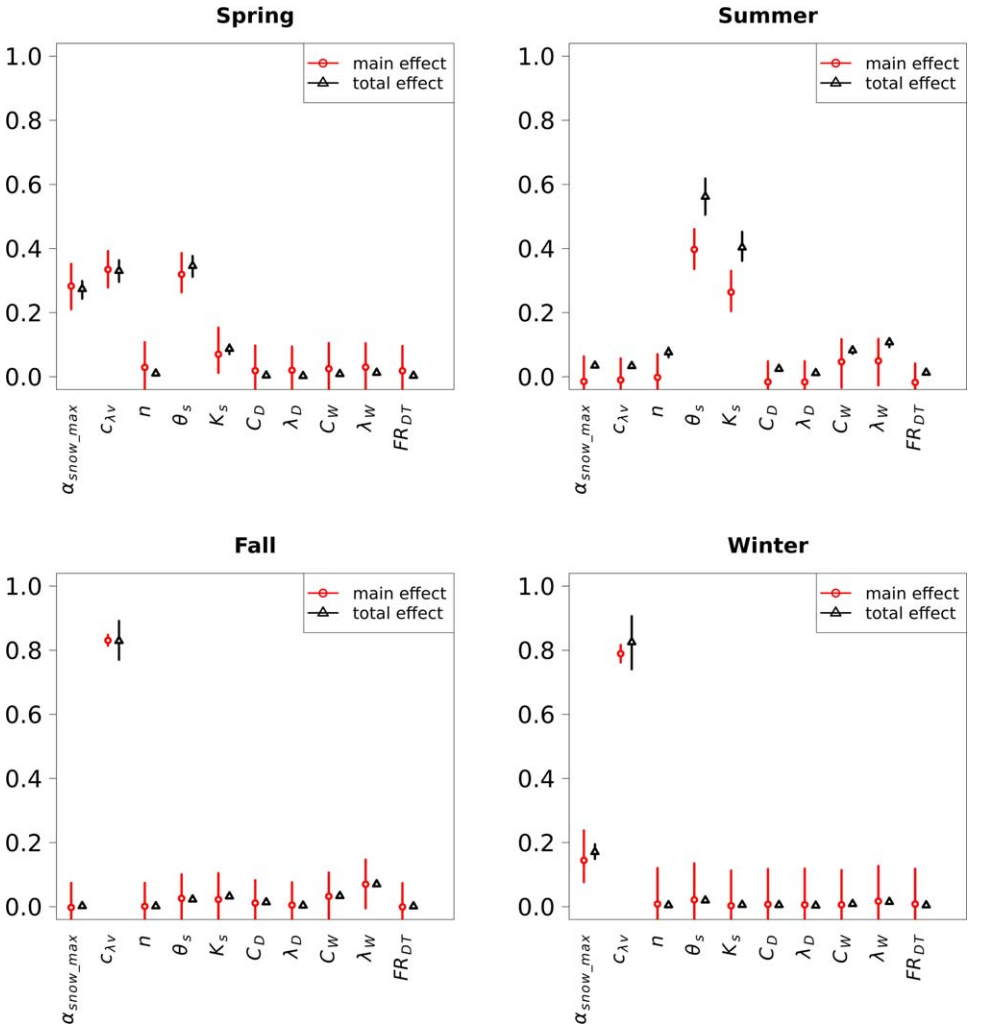

Figure 4. Total and first-order sensitivity indices on soil temperature for the most influential ORCHIDEE parameters (reduced parameter set).

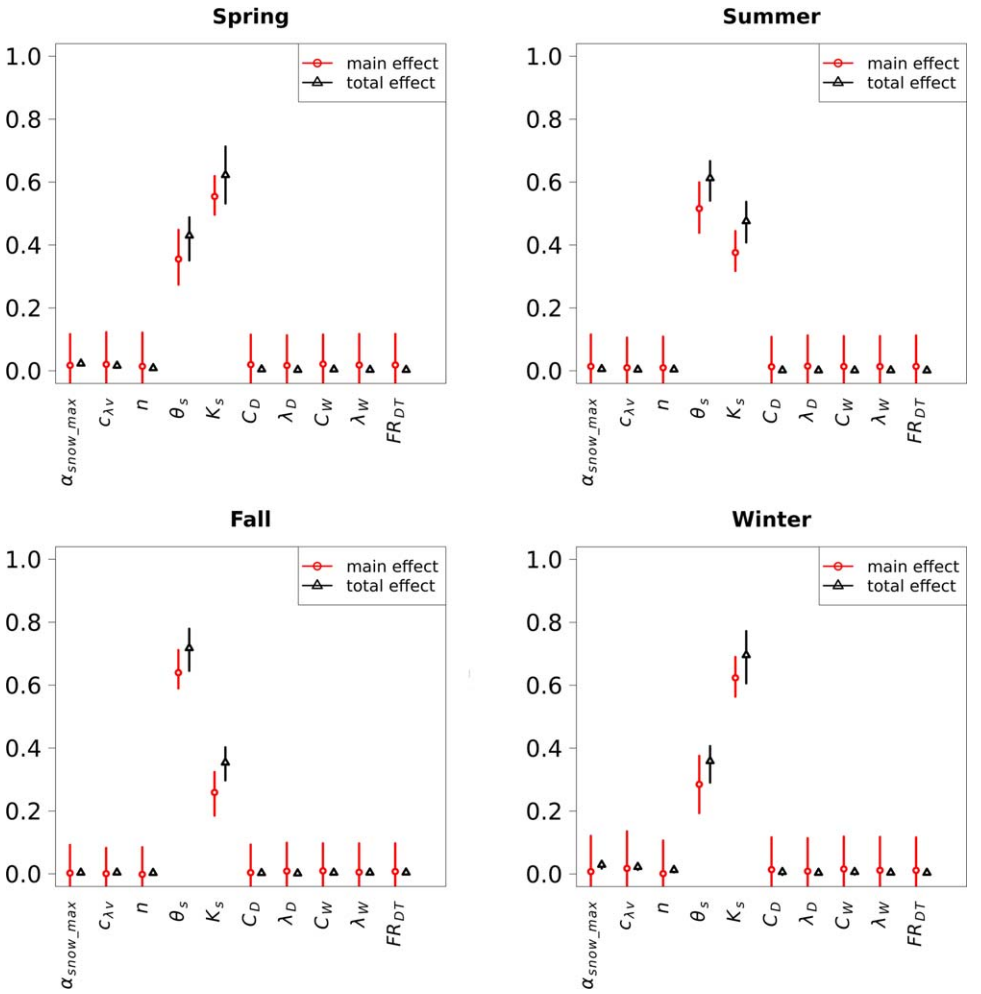

Figure 5. Total and first-order sensitivity indices on soil moisture for the most influential ORCHIDEE parameters (reduced parameter set).

parameter $C_{\lambda v}$. These parameters will be used in the model calibration process to tune the model to site observations.

5. Model Calibration

Model calibration was performed for both tundra and forest sites using the soil moisture, soil temperature and ALT observations acquired during the summer 2012 field experiment. The methodology was based on a simple OAT calibration procedure, by minimizing the model-data discrepancies. The calibration was first performed on the Θ_s, Θ_r, and K_s parameters, which influence both soil temperature and soil moisture; the calibration was then extended to the other parameters (i.e., λ_W, C_W, and $C_{\lambda v}$). In this calibration process, the same weight has been given to each observation. The range of variation of all the parameters subject to calibration and the calibrated values obtained are compared in Table 5 to the values prescribed in the standard ORCHIDEE version. The model simulations were performed with the meteorological forcing resulting from the merging of the in situ measurements with the ERA-INTERIM reanalysis data, as described in section 3.2, after a spin-up performed on years 2001–2011, provided by the ERA-INTERIM reanalysis only.

5.1. Forest Site

Figure 7 displays the soil temperature and soil moisture profiles observed and simulated for the forest site over the whole period of measurements, i.e., from early August to the end of October. The soil temperatures observations (in black) are all above freezing point down the whole profile during the experimental period, and show a negative (i.e., cooling) trend as expected in this period of the year (end of summer). The

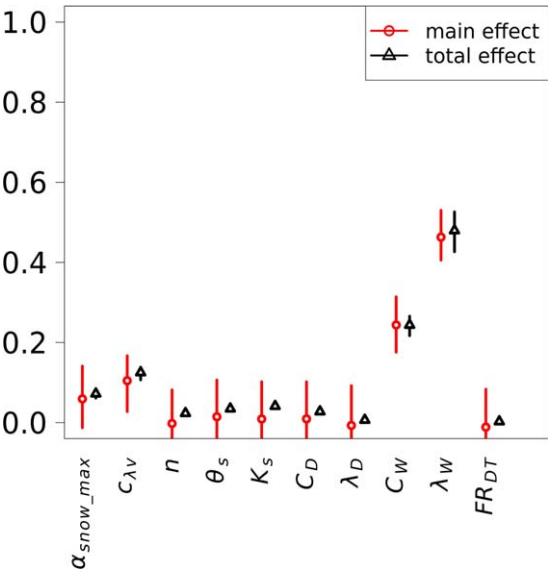

Figure 6. Total and first-order sensitivity indices on active layer thickness for the most influential ORCHIDEE parameters (reduced parameter set).

maximum value at 2 cm depth is 287.5 K in August and the minimum is 275 K in October. At 1 m depth, the soil is still unfrozen with temperatures larger than 276 K in October. The observed diurnal amplitudes are around 5 K at 2 cm, falling to 0.1 K at 50 cm and almost zero at 100 cm. The soil is quite dry, with soil moisture values around 0.15 $m^3\ m^{-3}$ in the top 30 cm; the soil is drier further down with values lower than 0.07 $m^3\ m^{-3}$ in the 50–100 cm soil layer. These features may be explained by the soil structure at the forest station: a soil layer with gravels and stones with grain size up to 2 cm is observed at least down to 80 cm in the sandy loam horizon. Such a soil texture presents a large hydraulic conductivity allowing deep infiltration. Therefore, after a rainfall event, the water is transferred directly to the water table and does not remain in the superficial soil layers. This explains the very low values of soil moisture observed in the 50–100 cm zone. The presence of mosses with their root system and vegetation residues in the litter, increases evapotranspiration (from the mosses) and water infiltration, which also contribute to the soil surface drying. The high soil temperatures and the nondetection of permafrost in the top 3 m may be the consequence of the soil dryness which prevents detection of the frozen horizon with the manual device (3 m length metal rods) used in this experiment. However, it could also indicate that our forest site is located on a talik. It has indeed been shown that the northwest of Siberia already shows thawing permafrost zones and formation of new taliks, especially in sandy sediments [*Romanovsky et al.*, 2010]; this change is a result of increased snow cover and a warming climate. The site location at the southern boundary of the continuous permafrost zone gives more plausibility to this second assumption.

If we compare the model simulations with the observations, Figure 7 shows that ORCHIDEE reproduces these quite well when using its standard parameterizations (blue curves). The soil temperatures are in very good agreement at all depths with a small cold bias of about 1 K increasing in the fall and an RMSE (root-mean-square error) less than 1.6 K. The diurnal amplitudes are also well simulated all along the period and at each depth. The soil moisture is also well simulated on average in the first top 20 cm of soil, but the discrepancies increase with depth (wet bias) showing that the model is unable to simulate the soil dryness observed below. It is also shown that the model simulates a more dynamic water content in the top first 20 cm, with significant response to rainfall events, not visible in the observations.

On the same plots, the results after model calibration are drawn in red. The calibration consisted of tuning the soil moisture saturation and residual values, the hydraulic conductivity and the thermal coefficients (soil heat capacity and thermal conductivity). The best fit was obtained for the values shown in Table 5 by

Table 5. Standard and Calibrated Values of the ORCHIDEE Parameters Used For the Forest and the Tundra Simulations[a]

Forest	Standard	Calibrated	Range	Tundra	Standard	Calibrated	Range
Θ_s	0.41	0.43	0.4–0.53	Θ_s	0.43	0.43	0.4–0.53
Θ_r	0.056	0.065	0.03–0.1	Θ_r	0.078	0.04	0.03–0.1
K_s	1060	1200	50–1500	K_s	249	996–62–249	50–1500
λ_W	1.89	4.75	0.1–5	λ_W	1.89	0.17–0.17–1.89	0.1–5
λ_D	0.4	1	0.01–5	λ_D	0.4	0.04–0.04–0.4	0.01–5
$C_{\lambda v} \times (-1)$	290	290	232–348	$C_{\lambda v} \times (-1)$	290	290	232–348
$C_D \times 10^{-6}$	1.8	1.8	1.8–8.4	$C_D \times 10^{-6}$	1.8	0.16–0.14–1.8	0.1–8.4
$C_W \times 10^{-6}$	3.03	3.	2.4–10	$C_W \times 10^{-6}$	3.03	0.27–0.24–3	0.2–9

[a]The range of variations prescribed for the calibration task is also indicated. For the Tundra site, the three calibrated values correspond to the three soil horizons prescribed (0–4.5, 4.5–18.6, and 18.6–9000 cm).

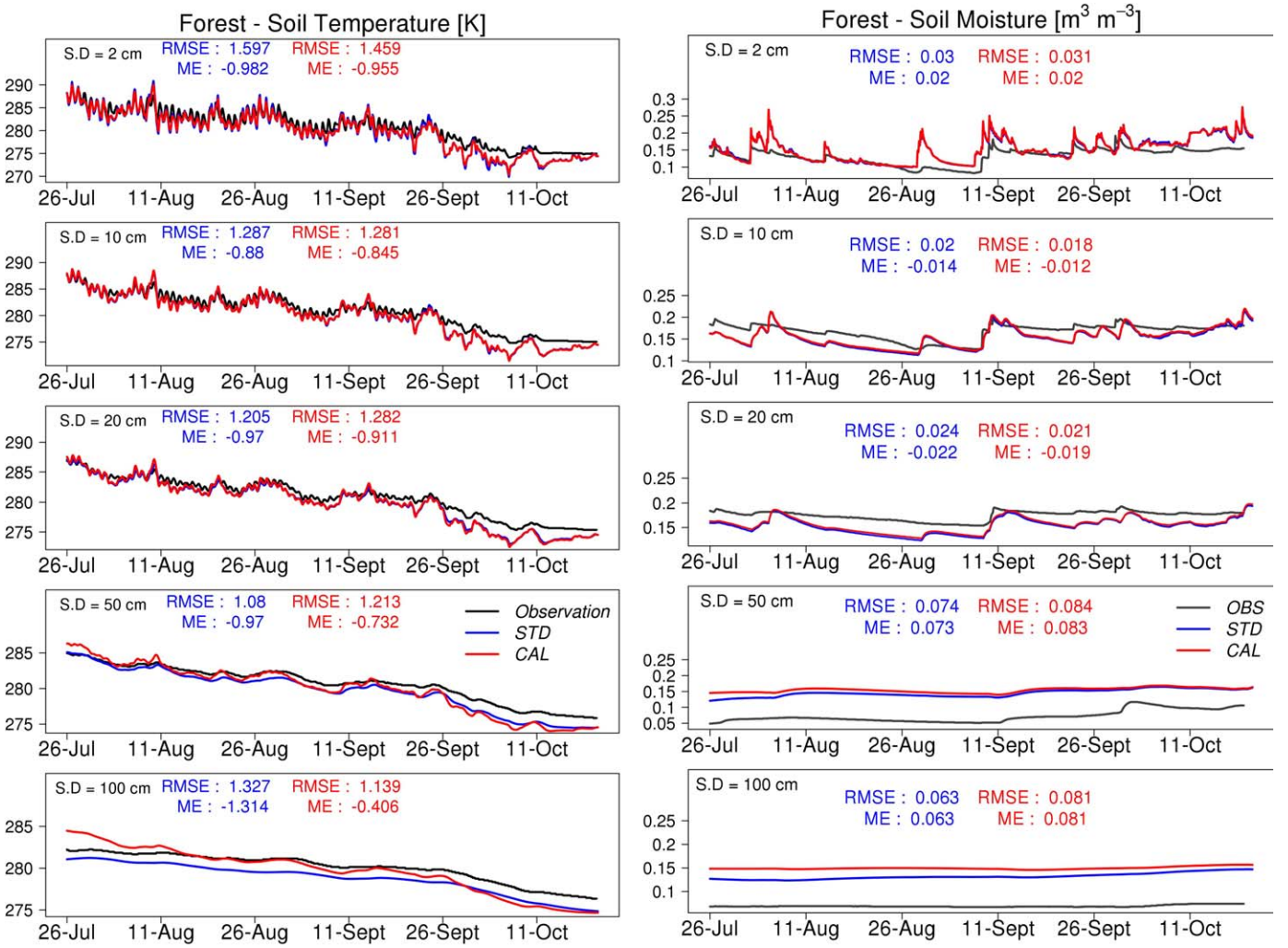

Figure 7. Comparison of simulated soil temperature (K) and simulated soil moisture ($m^3\ m^{-3}$) at different soil depths (S.D.: 2, 10, 20, 50, and 100 cm) for the Forest site. The standard (STD, in blue) and calibrated (CAL, in red) ORCHIDEE simulations are plotted against observations (in black). RMSE and bias (mean error; ME) are indicated in the corresponding color.

slightly increasing the hydraulic conductivity at saturation (by about 10%, from 1060 to 1200 mm d^{-1}) and by increasing the soil thermal conductivity by a factor of 1.5. The soil heat capacity and the snow parameters were not changed in the calibration process, the standard values giving the best fit. The soil thermal and hydrological conductivities (before and after calibration) are plotted in supporting information Figure S1 on the same period. Even if the response to rainfall events is still overemphasized in the simulations, the improvements obtained on soil moisture above 20 cm depth are clearly visible by the reduction of the biases and RMSEs by a factor of about 15%. The biases and the RMSEs are slightly increased by factors of 20% and 30% at 50 and 100 cm, respectively. The simulation of a drier soil and the larger heat conductivity in particular lead to a slight increase of the soil temperature, which becomes closer to the observations especially below 20 cm. For example, the cold bias at 100 cm is reduced by 0.6 K and is close to 0 if the fall period is removed. Indeed, the model is not able to reproduce the soil temperatures observed during this time period, whatever the depth. This issue seems to be linked to an underestimation of the LAI for this forested site whose value falls to 0 at the end of September in the model. Comparison with satellite measurements shows that some vegetation is still present at this time of the year. The incorrect representation of the vegetation senescence in the model may explain the too rapid cooling due to the nonrepresentation of the insulation effect which impacts significantly the turbulent transfers in the boundary surface layer. A better parameterization of the vegetation seasonal variations and of the forest understorey should improve our results. Anyway, the ALT modeled with this calibrated version is also in agreement with the

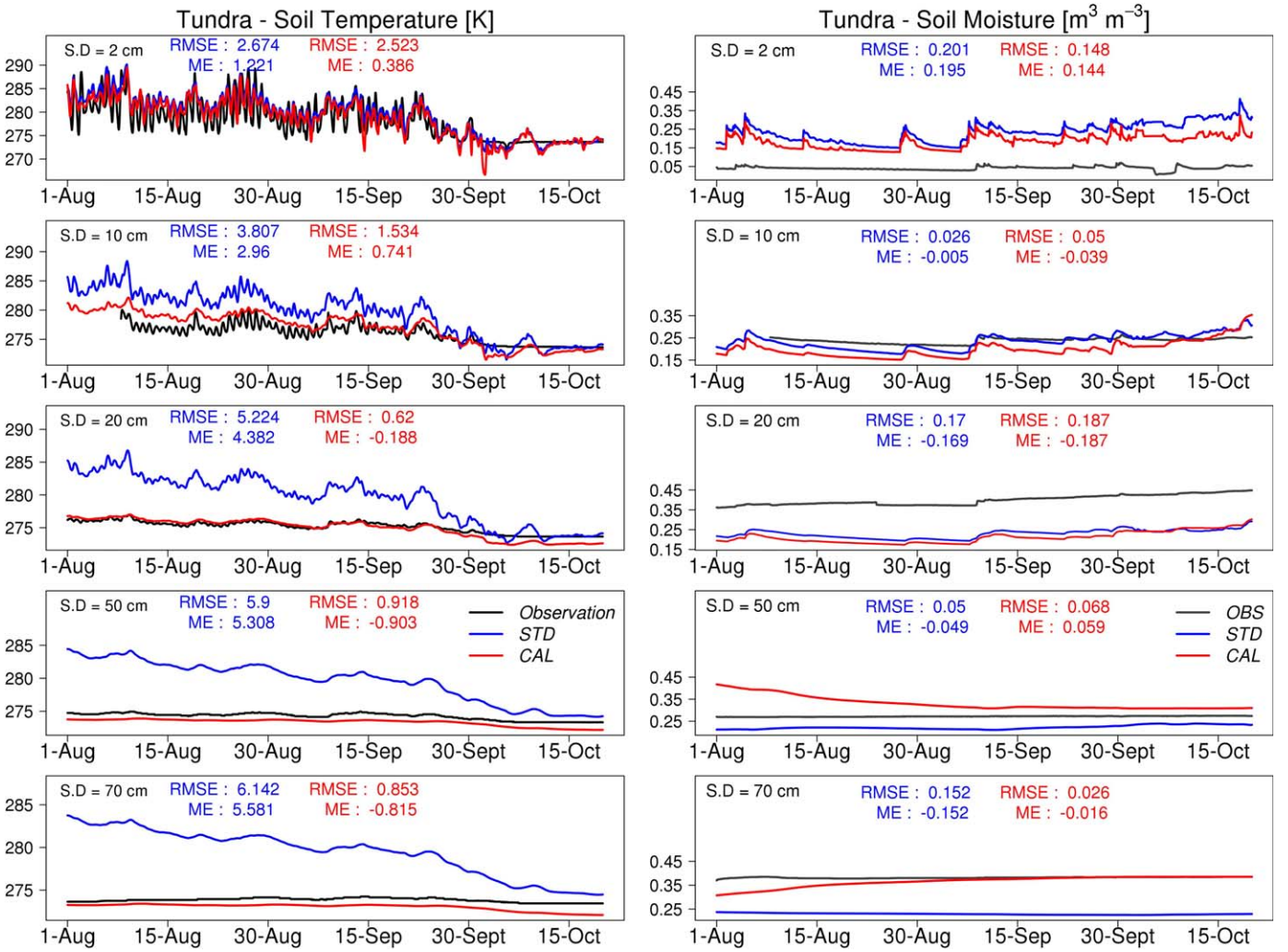

Figure 8. Comparison of simulated soil temperature (K) and soil moisture ($m^3\ m^{-3}$) at different soil depths (S.D.: 2, 10, 20, 50, and 70 cm) for the Tundra site. The standard (STD, in blue) and calibrated (CAL, in red) ORCHIDEE simulations are plotted against observations (in black). RMSE and bias (mean error; ME) are indicated in the corresponding color.

observations with a simulated value of 500 cm in line with the in situ measurements. This result shows that with our atmospheric forcing data and sandy soil thermal conditions, the model is able to simulate the soil temperatures and the absence of permafrost in the first 5 m. Such a result supports the hypothesis that our site is probably situated on a newly formed talik.

5.2. Tundra Site

The soil temperature and moisture profiles observed and simulated for the tundra site are displayed in Figure 8. The observations (in black) show clearly lower temperatures compared to the forest site, by 5 K on average, larger diurnal-cycle amplitude at the surface and larger attenuation with depth. Indeed, at 2 cm depth, the diurnal cycle shows temperature amplitudes that are comparable to the air temperature diurnal variations (not shown here). The top of the permafrost is clearly visible for the tundra site, lying in summer at around 70 cm depth, close to the averaged ALT measurements giving an average value of 61.2 ± 7.2 cm (calculated on 100 samples). The soil surface is completely dry (explaining the large diurnal temperature variations observed), but soil moisture increases with depth.

If we compare these observations to the results of the ORCHIDEE simulation with its standard parameterization (blue curves), the plots show that the model generally overestimates the soil temperature with a positive bias of about 1.2 K at the surface and larger than 5 K at 70 cm. The model is therefore unable to

simulate the top of the permafrost. The soil moisture is also overestimated at the surface (positive bias of 0.2 m^3 m^{-3}) and underestimated below 10 cm depth (biases are ranging between −0.05 and −0.17 m^3 m^{-3} depending on the soil layers monitored).

These results show clearly that in the tundra case, contrary to the forest site, vertically uniform values of the hydrothermal properties will never lead to a better fit to the observations either at the surface or below, because the biases are in opposite directions. For example, increasing the hydraulic conductivity will likely improve the surface conditions but degrade the deeper soil. The thermodynamic calibration is more promising and a better fit is expected with a reduction of the thermal conductivity which will allow the model to decrease the soil heating and the soil temperatures in summer.

As already noted in section 2, the soil of the tundra site is more complex than the forest site and presents different horizons. An organic layer is situated between 5 and 15 cm below a sandy loam layer of 5 cm depth containing many residues of green moss and sphagnum. These conditions can explain the dryness of the top centimeters and the high levels of soil water content below. The moss vegetation and the organic layer contribute both to the soil insulation and explain the smaller thickness of the active layer compared to the forest site. To model such a configuration, we propose to benefit from the recent vertical discretization of the thermal properties in ORCHIDEE and to represent the vertical heterogeneity of the soil properties using the new parameterization proposed by *Wang et al*. [2016]. This model will represent the soil in a multihorizon configuration, distinguishing three media: the top layer (first five layers in the model) from the surface to 4.5 cm well drained, a transition layer down to 18.6 cm presenting lower heat and hydraulic conductivities (represented by the layers 6 and 7) supposed to mimic a peat/organic soil, and the silty loam soil below (layers 8–18). For each of these three layers, soil properties have been calibrated and the results are indicated in Table 5. In the calibration, only the hydraulic and thermal conductivity were changed: the thermal conductivity was decreased by a factor of about 10 for the seven first layers and the hydraulic conductivity was increased by a factor of 4 in the first five layers to account for the specific draining properties of the moss layers, and it was decreased by a factor of 4 in the layers 6 and 7, to represent the peat layer and its high water storage and low infiltration [*Päivänen*, 1973]. The remaining soil below was set to the silty loam standard values.

The simulated soil temperature and moisture with this new model and these calibrated values are shown in Figure 8 in red. Supporting information Figure S2 presents the simulated soil thermal and hydraulic conductivities (before and after calibration), plotted for the same period. It can be seen that the introduction of vertical variability in the thermal and hydraulic properties corrects the soil moisture biases (decrease at the surface and increase below the peat/organic layer). The soil temperature simulation is also much improved by the reduction of the thermal conductivity; the agreement with the observations here is indeed remarkable. The mean errors are reduced significantly by several degrees (by a factor of 3 at the surface to a factor of 5 more deeply), but being always less than 1 K. The RMSEs have been also much reduced and are about 2.5 K at the surface, and less than 1 K below the depth of 20 cm. Moreover, the model is now able to simulate the top of the permafrost with a simulated ALT of 57 cm close to the observations equal to 61 ± 7 cm. Concerning soil moisture, the errors are also reduced in the calibrated simulation, the mean error is reduced by a factor 1.4 at the surface and by a factor 10 at the depth of 70 cm, the RMSEs are less than 0.2 K at all levels. Therefore, even if the observation errors are larger for this site compared to the forest one because of the colder temperatures, as already mentioned, the model now succeeds in representing the vertical features of the soil moisture and temperature. These improvements demonstrate the benefit of the new soil vertical discretization which allows us to prescribe different properties to each soil layer and therefore to improve the representation of the multiple soil horizons often observed in cryospheric environments.

6. Conclusions

This paper presents an application of the ORCHIDEE land surface model at local scale on two experimental sites located in the Siberian Arctic zone. The comparison between model results and observations was carried out after performing a global sensitivity analysis focused on ALT, soil temperature, and moisture output variables. This analysis was performed in two steps: a first step based on the Morris screening approach permitted us to select the most sensitive parameters (10 out of the 48 model parameters). This reduced

parameter set was analyzed in a second step based on a full analysis of the variance following the Sobol' approach. The methodology appears very efficient at identifying the sensitive parameters within the whole parameter space with a limited number of simulations. It also allows the parameter sensitivities for each studied output variable to be ranked. The results show that the saturated soil water content Θ_s and the hydraulic conductivity at saturation K_s are the most sensitive parameters impacting summer soil temperature and moisture content and that the soil thermal conductivity λ_W, the heat capacity C_w and the snow thermal conductivity parameter $C_{\lambda v}$ also show significant impact on the simulation of summer soil temperature. These parameters have been calibrated for the two sites under study and the model simulations have been compared to the observations. The results were discussed in relation to the field measurements and soil description available. They highlight the skill of the ORCHIDEE model at representing the soil moisture and temperature profiles in both cases of an homogeneous soil (forest site) and a multiple horizons one (tundra site). The thermal insulation of the organic matter [*Rinke et al*., 2008], of the vegetation and especially of mosses [*Beringer et al*., 2001] and their impact on insulation and infiltration properties have been identified as key processes that need to be represented in cryospheric environments. The new vertical discretization in ORCHIDEE provides a method of representing the complexity of Arctic soils by accounting for the vertical variability of the soil hydraulic and thermal properties. In our case, the local observations permitted us to improve the representation of this heterogeneity for the tundra site, but the extension to larger scales requires more developments if we are to maintain the link with the carbon cycle and other trace gas processes not investigated in this study. Soil organic matter and its impacts on soil thermal and hydraulic properties need to be explicitly parameterized. The ORCHIDEE team is now working to account for the organic part of soils in the modeling of the thermal and hydraulic conductivities and capacities, as well as soil porosity and water holding capacity.

The representation of mosses in the Arctic environment is also a subject that requires further development. Their impacts on soil thermodynamics and hydrology, and more widely on the energy, water, and carbon balances, have been demonstrated, and their representation in climate models should be a priority to improve the modeling of soil temperatures and permafrost evolution under a warming climate. Such developments are also under study in our team (A. Druel, personal communication, 2016).

The need to run long-term simulations of past climates to better initialize the permafrost extent and temperatures has also been highlighted and requires attention. In this study, the lack of long-term forcing data and identified biases between atmospheric forcing data sets, led to uncertainties in the soil temperature initialization and could have biased the deep soil temperatures. These biases had no consequences here because our study was focused on surface processes and on short-term evaluation. Therefore, deep soil temperature errors did not impact surface transfers, but if long-term processes were to be studied, such errors would no longer be negligible.

Finally, this work allowed us to test ORCHIDEE in tundra environments on experimental sites that have made available both soil moisture and temperature profiles. These data allow us to perform model parameter sensitivity analyses and to identify model weaknesses but are clearly not sufficient to fully calibrate and evaluate the modeling of soil water movement. The lack of long-term data series (at least over a full year) limited the number of parameters and processes to calibrate. The lack of some local meteorological data, especially snow/rain partitioning and radiation (upwelling and downwelling for albedo assessment), which can show large spatial variability, limited also the calibration and evaluation potential and further model developments. The development of Arctic experimental sites dedicated to the long-term monitoring of the energy and mass transfers in the atmosphere-biosphere continuum is therefore crucial for land surface modeling and prediction improvements. This work has shown how, for both soil moisture and temperature, field measurements can be used to calibrate the soil thermal and hydraulic processes which are strongly linked. Flux measurements would have helped even more to evaluate and calibrate albedo and evapotranspiration resistances for instance. High frequency measurements (hourly data) are also required to evaluate the diurnal cycles and such devices and experimental setups should be supported.

At larger scale, spaceborne-dedicated instruments also help by mapping and monitoring soil thermal and hydraulic states, and how they are responding to changing vegetation and climate. Such data are vital in evaluating and calibrating land surface models. Earth-monitoring satellite programs require continuing commitment and funding.

Acknowledgments
The authors are grateful to the WSIBISO project funded by the Russian Federation under contract 11.G34.31.0064 and to the French ANR CLASSIQUE project (ANR Grant No. ANR 2010-CEPL-012-02), for funding this study. They acknowledge also J. Polcher and C. Grenier for fruitful discussions as well as anonymous reviewers for their valuable comments and suggestions that improved the quality of our manuscript. The source code for the model used in this study, the IPSL-ORCHIDEE, is freely available at http://labex.ipsl.fr/orchidee/. Both the data and input files necessary to reproduce the experiments are available from the authors upon request (catherine.ottle@lsce.ipsl.fr). The data are archived at the Laboratoire des Sciences du Climat et de l'Environnement (LSCE).

References

Belward, A., J. Estes, and K. Kline (1999), The IGBP-DIS Global 1-km Land-Cover Data Set DISCover: A project overview, *Photogramm. Eng. Remote Sens.*, *9*, 1013–1020.

Benavidès Pinjosovsky, H. S., S. Thiria, C. Ottlé, J. Brajard, F. Badran, and P. Maugis (2017), Variational assimilation of land surface temperature within the ORCHIDEE Land Surface Model Version 1.2.6, *Geosci. Model Dev.*, *10*, 85–104, doi:10.5194/gmd-10-85-2017.

Beringer, J., A. H. Lynch, F. S. Chapin III, M. Mack, and G. B. Bonan (2001), The representation of Arctic soils in the land surface model: The importance of mosses, *J. Clim.*, *14*(15), 3324–3335.

Bicheron, P., M. Leroy, C. Brockmann, U. Krämer, B. Miras, M. Huc, and D. Gross (2006), Globcover: A 300 m global land cover product for 2005 using ENVISAT MERIS time series, in *Proceedings of the Second International Symposium on Recent Advances in Quantitative Remote Sensing*, pp. 538–542, Serv. de Publ., Univ. de Valencia, Valencia, Spain.

Bontemps, S., et al. (2013), Consistent global land cover maps for climate modelling communities: Current achievements of the ESA's land cover CCI, paper presented at the ESA Living Planet Symposium, Edinburgh, U. K., 9–13 Sept.

Campolongo, F., J. Cariboni, and A. Saltelli (2007), An effective screening design for sensitivity analysis of large models, *Environ. Modell. Software*, *22*(10), 1509–1518.

Campolongo, F., A. Saltelli, and J. Cariboni (2011), From screening to quantitative sensitivity analysis: A unified approach, *Comput. Phys. Commun.*, *182*(4), 978–988.

Carsel, R. F., and R. S. Parrish (1988), Developing joint probability distributions of soil water retention characteristics, *Water Resour. Res.*, *24*(5), 755–769.

Chadburn, S., E. Burke, R. Essery, J. Boike, M. Langer, M. Heikenfeld, P. Cox, and P. Friedlingstein (2015), An improved representation of physical permafrost dynamics in the JULES land-surface model, *Geosci. Model Dev.*, *8*(5), 1493–1508.

Chapin, F. S., et al. (2005), Role of land-surface changes in Arctic summer warming, *Science*, *310*(5748), 657–660.

Dankers, R., E. J. Burke, and J. Price (2011), Simulation of permafrost and seasonal thaw depth in the JULES land surface scheme, *Cryosphere*, *5*(3), 773–790.

De Rosnay, P., J. Polcher, M. Bruen, and K. Laval (2002), Impact of a physically based soil water flow and soil-plant interaction representation for modeling large-scale land surface processes, *J. Geophys. Res.*, *107*(D11), doi:10.1029/2001JD000634.

Dickinson, R. E., A. Henderson-Sellers, and P. J. Kennedy (1993), Biosphere-atmosphere Transfer Scheme (BATS) Version 1e as Coupled to the NCAR Community Climate Model, *Rep. N. T. N. NCAR/TN-387+STR*, Boulder, Colo.

Ducoudré, N., K. Laval, and A. Perrier (1993), SECHIBA, a new set of parameterizations of the hydrologic exchanges at the land-atmosphere interface within the LMD Atmospheric General Circulation Model, *J. Clim.*, *6*(2), 248–273.

Dufresne, J. L., et al. (2013), Climate change projections using the IPSL-CM5 Earth System Model: From CMIP3 to CMIP5, *Clim. Dyn.*, *40*(9–10), 2123–2165.

Frolov, I. E., I. M. Ashik, H. Kassens, I. V. Polyakov, A. Y. Proshutinsky, V. T. Sokolov, and L. A. Timokhov (2009), Anomalous variations in the thermohaline structure of the Arctic Ocean, *Dokl. Earth Sci.*, *429*(2), 1567–1569.

Gouttevin, I., G. Krinner, P. Ciais, J. Polcher, and C. Legout (2012), Multi-scale validation of a new soil freezing scheme for a land-surface model with physically-based hydrology, *Cryosphere*, *6*(2), 407–430.

Groisman, P., and A. J. Soja (2009), Ongoing climatic change in Northern Eurasia: Justification for expedient research, *Environ. Res. Lett.*, *4*(4), 045002, doi:10.1088/1748-9326/4/4/045002.

Groisman, P. Y., T. R. Karl, R. W. Knight, and G. L. Stenchikov (1994), Changes of snow cover, temperature, and radiative heat balance over the Northern Hemisphere, *J. Clim.*, *7*(11), 1633–1656.

Gubler, S., S. Endrizzi, S. Gruber, and R. S. Purves (2013), Sensitivities and uncertainties of modeled ground temperatures in mountain environments, *Geosci. Model Dev.*, *6*(4), 1319–1336.

Guglielmo, F., et al. (2015), Simulating hydrology with an isotopic land surface model in western Siberia: What do we learn from water isotopes?, *Hydrol. Earth Syst. Sci. Discuss.*, *12*, 9393–9436.

Hinzmann, L. D., et al. (2005), Evidence and implications of recent climate change in Northern Alaska and other Arctic regions, *Clim. Change*, *72*, 251–298.

Homma, T., and A. Saltelli (1996), Importance measures in global sensitivity analysis of nonlinear models, *Reliab. Eng. Syst. Safety*, *52*(1), 1–17.

Hourdin, F., et al. (2006), The LMDZ4 general circulation model: Climate performance and sensitivity to parametrized physics with emphasis on tropical convection, *Clim. Dyn.*, *27*, 787–813.

Jansen, M. J. W. (1999), Analysis of variance designs for model output, *Comput. Phys. Commun.*, *117*(1–2), 35–43.

Koenigk, T., L. Brodeau, R. Graversen, J. Karlsson, G. Svensson, M. Tjernström, U. Willén, and K. Wyser (2013), Arctic climate change in 21st century CMIP5 simulations with EC-Earth, *Clim. Dyn.*, *40*(11–12), 2719–2743.

Koven, C. D., B. Ringeval, P. Friedlingstein, P. Ciais, P. Cadule, D. Khvorostyanov, G. Krinner, and C. Tarnocai (2011), Permafrost carbon-climate feedbacks accelerate global warming, *Proc. Natl. Acad. Sci. U. S. A.*, *108*(36), 14,769–14,774.

Koven, C. D., W. J. Riley, and A. Stern (2013), Analysis of permafrost thermal dynamics and response to climate change in the CMIP5 Earth System Models, *J. Clim.*, *26*(6), 1877–1900.

Krinner, G., N. Viovy, and N. De Noblet-Ducoudré (2005), A dynamic global vegetation model for studies of the coupled atmosphere-biosphere system, *Global Biogeochem. Cycles*, *19*, GB1015, doi:10.1029/2003GB002199.

Kuppel, S., F. Chevallier, and P. Peylin (2013), Quantifying the model structural error in carbon cycle data assimilation systems, *Geosci. Model Dev.*, *6*, 45–55.

Loranty, M. M., and S. J. Goetz (2012), Shrub expansion and climate feedbacks in Arctic tundra, *Environ. Res. Lett.*, *7*(1), 011005.

Lu, X., Y.-P. Wang, T. Ziehn, and Y. Dai (2013), An efficient method for global parameter sensitivity analysis and its applications to the Australian community land surface model (CABLE), *Agric. For. Meteor.*, *182–183*(0), 292–303.

Morris, M. D. (1991), Factorial sampling plans for preliminary computational experiments, *Technometrics*, *33*(2), 161–174.

Nicolsky, D. J., V. E. Romanovsky, V. A. Alexeev, and D. M. Lawrence (2007), Improved modeling of permafrost dynamics in a GCM land-surface scheme, *Geophys. Res. Lett.*, *34*, L08501, doi:10.1029/2007GL029525.

Nossent, J., P. Elsen, and W. Bauwens (2011), Sobol' sensitivity analysis of a complex environmental model, *Environ. Modell. Software*, *26*(12), 1515–1525.

Olson, J., J. Watts, and L. Allison (1983), Carbon in live vegetation of major world ecosystems, *Tech. Rep. W-7405-ENG-26*, 152 pp., Oak Ridge Natl. Lab., Oak Ridge, Tenn.

Ottlé, C., J. Lescure, F. Maignan, B. Poulter, T. Wang, and N. Delbart (2013), Use of various remote sensing land cover products for PFT mapping over Siberia, *Earth Syst. Sci. Data*, *5*, 331–348.

Päivänen, J. (1973), *Hydraulic Conductivity and Water Retention in Peat Soils*, Suomen Metsätieteellinen Seura, Helsinki, Finland.
Paquin, J. P., and L. Sushama (2015), On the Arctic near-surface permafrost and climate sensitivities to soil and snow model formulations in climate models, *Clim. Dyn.*, *44*(1–2), 203–228.
Peng, S., et al. (2016), Simulated high-latitude soil thermal dynamics during the past 4 decades, *Cryosphere*, *10*, 179–192, doi:10.5194/tc-10-179-2016.
Pujol, G., B. looss, and M. B. looss (2014), *Package 'Sensitivity', R Package Version 1.8–2*. [Available at http://CRAN.R-project.org/package=sensitivity.]
Rinke, A., P. Kuhry, and K. Dethloff (2008), Importance of a soil organic layer for Arctic climate: A sensitivity study with an Arctic RCM, *Geophys. Res. Lett.*, *35*, L13709, doi:10.1029/2008GL034052.
Romanovsky, V. E., et al. (2010), Thermal state of permafrost in Russia, *Permafrost Periglac. Process.*, *21*, 136–155.
Saltelli, A. (2002), Making best use of model evaluations to compute sensitivity indices, *Comput. Phys. Commun.*, *145*(2), 280–297.
Saltelli, A., M. Ratto, T. Andres, F. Campolongo, J. Cariboni, D. Gatelli, M. Saisana, and S. Tarantola (2008), *Global Sensitivity Analysis: The Primer*, John Wiley, Hoboken, N. J.
Saltelli, A., P. Annoni, I. Azzini, F. Campolongo, M. Ratto, and S. Tarantola (2010), Variance based sensitivity analysis of model output, Design and estimator for the total sensitivity index, *Comput. Phys. Commun.*, *181*(2), 259–270.
Serreze, M. C., A. P. Barrett, A. G. Slater, M. Steele, J. L. Zhang, and K. E. Trenberth (2007), The large-scale energy budget of the Arctic, *J. Geophys. Res.*, *112*, D11122, doi:10.1029/2006JD008230.
Sitch, S., et al. (2003), Evaluation of ecosystem dynamics, plant geography and terrestrial carbon cycling in the LPJ dynamic global vegetation model, *Global Change Biol.*, *9*(2), 161–185.
Slater, A. G., and D. M. Lawrence (2013), Diagnosing present and future permafrost from climate models, *J. Clim.*, *26*(15), 5608–5623.
Sobol, I. M. (1990), On sensitivity estimation for nonlinear mathematical models [in Russian], *Mat. Model.* [*Math. Model. Comput. Exp.*, Engl. Transl., *2*(1), 112–118.]
Sobol, I. M. (2001), Global sensitivity indices for nonlinear mathematical models and their Monte Carlo estimates, *Math. Comput. Simul.*, *55*, 271–280.
Valdayskikh, V., O. Nekrasova, J. Jouzel, A. Uchaev, and T. Radchenko (2013), Some characteristics of forest-tundra (West Siberia) soil groups distinguished on the basis of thermal properties, *Prace Geogr.*, *135*, 73–86, doi:10.4467/20833113PG.13.024.1552.
Vérant, S., K. Laval, J. Polcher, and M. De Castro (2004), Sensitivity of the continental hydrological cycle to the spatial resolution over the Iberian Peninsula, *J. Hydrometeorol.*, *5*, 267–285.
Wang, F., F. Cheruy, and J. L. Dufresne (2016), The improvement of soil thermodynamics and its effects on land surface meteorology in the IPSL climate model, *Geosci. Model Dev.*, *9*, 363–381, doi:10.5194/gmd-9-363-2016.
Wang, T., C. Ottlé, A. Boone, P. Ciais, E. Brun, S. Morin, G. Krinner, S. Piao, and S. Peng (2013), Evaluation of an improved intermediate complexity snow scheme in the ORCHIDEE land surface model, *J. Geophys. Res. Atmos.*, *118*, 6064–6079, doi:10.1002/jgrd.50395.